An observational study of the carbon-sink strength of East Asian subtropical evergreen forests

Zheng-Hong Tan[1,2,3]**, Yi-Ping Zhang**[1,3]**, Naishen Liang**[2]**, Yue-Joe Hsia**[4]**, Yong-Jiang Zhang**[1]**, Guo-Yi Zhou**[5]**, Yue-Lin Li**[5]**, Jehn-Yih Juang**[6]**, Hou-Sen Chu**[9]**, Jun-Hua Yan**[5]**, Gui-Rui Yu**[7]**, Xiao-Min Sun**[7]**, Qin-Hai Song**[1,8]**, Kun-Fang Cao**[1]**, D A Schaefer**[1] **and Yu-Hong Liu**[1,2]

[1] Key Laboratory of Tropical Forest Ecology, Xishuangbanna Tropical Botanical Garden, Chinese Academy of Sciences, Menglun 666303, People's Republic of China
[2] Center for Global Environmental Research, National Institute for Environmental Studies, Tsukuba 305-8506, Japan
[3] Ailaoshan Station for Subtropical Forest Ecosystem Studies, Chinese Ecosystem Research Network, Jingdong 676209, People's Republic of China
[4] Institute of Natural Resources, National Dong Hwa University, Hualien 10974, Taiwan
[5] South China Botanical Garden, Chinese Academy of Sciences, Guangzhou 510650, People's Republic of China
[6] Department of Geography, National Taiwan University, Taipei 10617, Taiwan
[7] Institute of Geographic Sciences and Natural Resources Research, Chinese Academy of Sciences, Beijing 100101, People's Republic of China
[8] Graduate University of Chinese Academy of Sciences, Beijing 100049, People's Republic of China
[9] Department of Environmental Sciences, The University of Toledo, Toledo, OH 43606-3390, USA

E-mail: yipingzh@xtbg.ac.cn

Abstract
Relatively little is known about the effects of regional warming on the carbon cycle of subtropical evergreen forest ecosystems, which are characterized by year-round growing season and cold winters. We investigated the carbon balance in three typical East Asia subtropical evergreen forests, using eddy flux, soil respiration and leaf-level measurements. Subtropical evergreen forests maintain continuous, high rates of photosynthetic activity, even during winter cold periods. Warm summers enhance photosynthetic rates in a limited way, because overall ecosystem productivity is primarily restrained by radiation levels during the warm period. Conversely, warm climates significantly enhance the respiratory carbon efflux. The finding of lower sensitivity of photosynthesis relative to that of respiration suggests that increased temperature will weaken the carbon-sink strength of East Asia subtropical evergreen forests.

1. Introduction

Predictions of global warming present an important question of how such climatic changes will affect ecosystem carbon balance. The Earth's average temperature has increased

0.74 °C in the past century (1906–2005) and is predicted to increase at an even faster rate (IPCC 2007). Forests store most of the carbon within the terrestrial ecosystem (∼1146 PgC based on inventory account (Dixon *et al* 1994)) and play an important role in global biogeochemical cycles, and will face an unprecedented warm climate. If warming induces additional release of carbon stored in forest ecosystems into the atmosphere, global warming will be accelerated (Cox *et al* 2000, Bond-Lamberty and Thomson 2010).

Although much work has been done to address this question, the results and potential outcomes are inconclusive. In contrast to grassland or tundra with lower canopy, it is very difficult to carry out whole-ecosystem-warming experiments in tall-canopy forests, whether using infrared heaters, buried heating cables or open-top chambers (Johnson *et al* 2000, Luo 2007). Most previous warming experiments in tall-canopy forest only examined warming of the soil rather than the whole ecosystem (Melillo *et al* 2002, Knorr *et al* 2005, Davidson and Jassens 2006). Whole-ecosystem-warming experiments, however, cannot be substituted by soil-warming experiments because there are interactions between soil and trees. For example, enhanced nitrogen availability, which benefits litterfall production and tree growth, was observed in a long-term soil-warming experiment (Melillo *et al* 2011).

Forest carbon balance response to warming scenarios will vary in different forest regions, elevations, and forest types. Global warming is predicted to increase tree growth of high-elevation forests but those at low elevations would show reduced growth (Latta *et al* 2010). Boreal and temperate tree growth was suggested to increase with increased temperature, in contrast to tropical forests (Way and Oren 2010). In practice, tree growth cannot represent ecosystem net carbon budget or even net primary production. Ecosystem net carbon budget accounting should include not only photosynthesis and autotrophic respiration of trees but also heterotrophic respiration of soil (Schulze 2006).

It is difficult to predict how ecosystem sink/source strength (termed net ecosystem production (NEP); Woodwell *et al* 1978) will respond to climate warming. As NEP is the small difference between gross primary production (GPP) and total ecosystem respiratory carbon loss (ER), a slight variation in GPP or ER could result in a significant effect on NEP. That is to say, it is more difficult to obtain a precise estimate for NEP than for GPP or ER. In reality, the response of NEP to climate warming is determined by the trade-off between the sensitivities of GPP and ER to increased temperature. If GPP is more sensitive than ER to warming, ecosystem NEP will increase, and vice versa.

Subtropical evergreen forests, known as 'oases on the Tropic of Cancer' are widespread in East Asia (Kira 1991). They represent the transition between temperate and tropical forests, with a year-around growing season and cold winter. The existence of subtropical forests completes a continuous spectrum of biomes (boreal, temperate, subtropical and tropical) within the terrestrial ecosystem. More than 200 million people in East Asia live in areas where subtropical evergreen forests exist or have existed in the past, and this ecosystem is the basis for the most active economy in the

region. However, these forests are facing strong pressures related to human disturbance and global climate change; unfortunately, little is known about the dynamics of these processes. The response of subtropical evergreen forests to elevated temperatures is especially poorly constrained, despite the ecological and human importance of this ecosystem. Warming will not affect subtropical evergreen forests in the same way that it affects temperate and boreal forests, because of the milder conditions and the year-round growing season (Piao *et al* 2008, Richardson *et al* 2010). It is also not known whether warming in subtropical evergreen forest ecosystems will have a negative impact on carbon uptake, as has been predicted for tropical forests (Way and Oren 2010), because subtropical evergreen forests occur in areas with pronounced cold winters, which is not the case in tropical regions.

This study incorporates eddy covariance flux observations, soil respiration, and leaf-level measurements to determine whether GPP or ER is more sensitive to climate warming in three typical subtropical evergreen forests in East Asia. We also examined why GPP or ER is more sensitive at these locations.

2. Materials and methods

2.1. Site descriptions

Three subtropical evergreen forests were chosen to investigate carbon balance response to regional warming at the ecosystem scale: Chilanshan in Taiwan (CLS); Dinghushan in Guangdong (DHS) and Ailaoshan in Yunnan (ALS) (table 1; figure 1). These three forests cover two monsoon types (East Asia Monsoon and Indian Monsoon), three stand ages (50, 100 and old growth more than 300 yr), three forest types (coniferous, broadleaf, and mixed) and three geographic locations (inland, far from sea; inland, near sea; and island). Details of the climate, vegetation, canopy and soil of these three forests were reported in previous studies (Chu 2008, Tan *et al* 2011, Wang *et al* 2006) and are not repeated here.

2.2. Eddy covariance observations

Two different research networks coordinate work on energy fluxes in the three study regions: the CLS site is maintained by TaiwanFLUX; DHS and ALS are parts of ChinaFLUX; both networks applied the same instruments for eddy flux observations. The open-path eddy covariance system comprised a CSAT-3 three-dimensional sonic anemometer (Campbell Scientific Inc., Logan, UT, USA) and a Li-7500 infrared gas analyzer (Li-Cor Inc., Lincoln, NE, USA). Data was collected at 10 Hz. Instrument height was related to mean canopy height (table 1). The dataset used in this study was collected during 2009. Flux data for DHS and ALS were processed using a procedure developed by ChinaFLUX, whereas CLS flux data were processed using the EdiRe micrometeorological software (University of Edinburgh). As the study assessed integration and comparison, we applied an identical data processing scheme for all three sites.
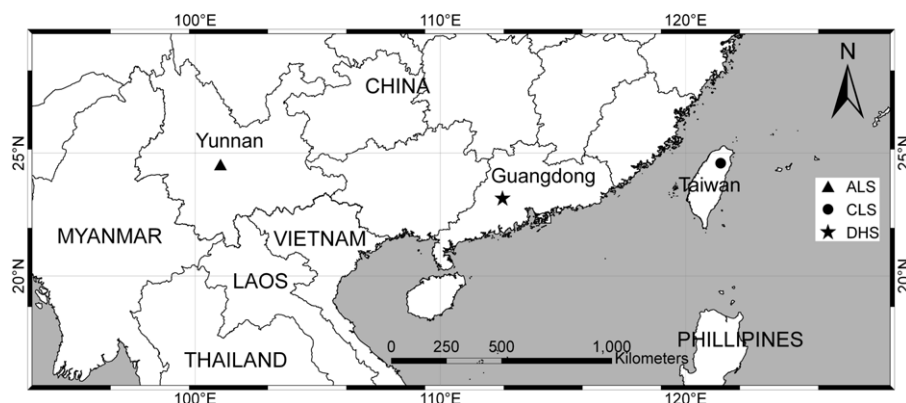
Figure 1. Geographic location of the study sites. The triangle, star and circle symbols indicate Ailaoshan (ALS), Dinghushan (DHS) and Chilanshan (CLS), respectively.

Table 1. Site descriptions.

Site	CLS	DHS	ALS
Location	24°35′28″N 121°25′56″E	23°10′24″N 112°32′10″E	24°32′17″N 101°01′44″E
Elevation of site (m)	1650	240	2502
MAT (°C)	14.7	21	11
PPT (mm)	4500	1956	1931
Sr (w m^{-2})	160	140	115
Predominate species	*Chamaecyparis obtusa var. formosana, Illicium anisatum, Dendropanax dentiger*	*Schima superba, Castanopsis chinensis, Pinus massoniana*	*Lithocarpus chintungensis, Rhododendron leptothrium, Vaccinium ducluoxii*
Canopy height (m)	12	17	26
Biomass (t ha^{-1})	162[a]	261	499
Forest type	Evergreen coniferous forest	Evergreen coniferous and broadleaved mixed forest	Evergreen broadleaved forest
Soil type	loamy Lithic Leptosol	loamy Lateritic Oxisol	loamy Alfisol
Z_r (m)	24	27	34
Monsoon type	East Asia monsoon	East Asia monsoon	Indian monsoon

[a] Biomass for this site represents data obtained for *Chamaecyparis obtusa var. formosana*, as this species comprises greater than 80% of the stand basal area (see Chang *et al* 2008). Z_r is the mounting height of the eddy covariance system. MAT is the mean annual temperature. PPT is the annual precipitation. Sr is mean solar radiation.

It is a convention, within the eddy flux community, to follow certain quality assurance and control (QA/QC) processes with eddy flux data before measurements are reported. For the present dataset, quality assurance steps, such as power spectral or co-spectra analysis with fast Fourier transform (FFT), flux-variance relationship test, energy balance closure calculation and footprint estimation, were carried out by previous studies (Chu 2008, Tan *et al* 2011, Wang *et al* 2006). In this study, we carried out the following QA/QC steps before obtaining the seasonal and annual average fluxes.

First, the averaging period covariance calculation is 30 min for all three sites.

Second, coordinate rotation (Tanner and Thurtell 1969) and WPL correction (Webb *et al* 1980) were applied to the flux dataset.

Third, the storage flux is included in estimating net ecosystem exchange, which derives from single-layer CO_2 data measured by Li-7500 (Hollinger *et al* 1994).

Fourth, any values exceeding 5.5 times standard deviation within a moving window of 10 values, or carbon fluxes outside the range $(-3, 3)$ (mg CO_2 m^{-2} s^{-1}), were regarded as spikes and were excluded from the analysis.

Fifth, u^*-filtering, gap-filling, and flux-partitioning were carried out using an online program maintained by the Max Planck Institute (www.bgc-jena.mpg.de/~MDIwork/eddyproc/index.php).

The nighttime flux data were previously criticized for low reliability due to calm air (Goulden *et al* 1996). Thus, the daytime data (defined as the period when photosynthetic active radiation (PAR) > 10 μmol m^{-2} s^{-1}) were used to represent light response at the leaf level (Goulden *et al* 1997). In this study, midday net ecosystem exchange (when PAR > 200) was also extracted (Goulden *et al* 2006) and was used to indicate temporal trend of photosynthesis capacity at the ecosystem level.

2.3. Soil efflux monitoring

Soil efflux measurement was conducted at the ALS site during October 2010 and September 2011. Twenty chambers were installed for four treatments (five replicates each):

3

Table 2. Ten most important evergreen broadleaf tree species selected for leaf-level measurements.

Species	Family
Lithocarpus jingdongensis Y C Hsu et H J Qian	Fagaceae
Symplocos sumuntia D Don	Symplocaceae
Vaccinium delavayi Franch	Vacciniaceae
Schima noronhae Reinw ex Blume	Theaceae
Manglietia insignis Blume	Magnoliaceae
Ternstroemia gymnanthera Sprague	Theaceae
Lithocarpus hypoviridis Y C Hsu, B S Sun et H J Qian	Fagaceae
Lyonia ovalifolia var. *lanceolata* Hand-Mazz	Ericaceae
Hartia sinensis Dunn	Theaceae
Illicium macranthum A C Smith	Illiciaceae

control, root cut, litterfall exclusion and warming. The control treatment data were used in this study. Soil efflux was monitored by a multichannel automated measurement system developed by Liang at the Japan National Institute for Environmental Studies (figure s1 available at stacks.iop.org/ERL/7/044017/mmedia). The system measured soil efflux in a flow-through and no-steady-state manner, and comprised 20 automatic chambers and a control box. The chambers (90 cm × 90 cm × 50 cm) are made from clear PVC. The system incorporates several design features to prevent gas outlet (Liang *et al* 2003). Two lids at the top of the chamber can be raised or closed, and are operated by compressed air (MAX-E-12, Techno Fronto) regulated by a four-way valve (BK120, Techno Fronto) (Liang *et al* 2003). Two fans (KMFH-12B, Kyoei, Tokyo, Japan) mounted in each chamber ensure sufficient mixing of air during measurement.

The main components of the control box are an infrared gas analyzer (IRGA, Li-840, Li-Cor Inc.) and a datalogger (CR10X, Campbell Scientific Inc.). During measurement, the air in the closed chamber is circulated through the IRGA by a micro-diaphragm pump (CM-50, Enomoto Ltd, Tokyo, Japan). The 20 chambers are closed sequentially by a home-made relay board controlled by the datalogger. The datalogger acquired outputs signals from the IRGA every 1 s and recorded average values every 10 s; the total sampling period for each chamber was 180 s. For each chamber, 1 efflux value was obtained per hour. The efflux was calculated from 18 records, as shown in equation (1):

$$R_{soil} = \frac{VP(1-W)}{RST} \frac{\partial c}{\partial t} \qquad (1)$$

where V is the volume of the chamber (m^3); S, the base area of the chamber (m^2); R, the gas constant (8.314 Pa m^3 K^{-1}); T, the air temperature in the chamber (K); P, air pressure (Pa); W, the water vapor mole fraction; and $\partial C/\partial t$, the rate of increase of CO_2 mole fraction (μmol mol^{-1} s^{-1}) in the chamber, calculated by the least-square method.

Soil temperature at 5 cm depth, and air temperature inside each chamber were measured with self-made thermocouples. Soil moisture at 10 cm was monitored with time-domain reflectometers (TDR) (CS616, Campbell Scientific Inc.). Air pressure at 30 cm height in the center of the plot was measured by a pressure transducer (PX2760, Omega Engineering, Inc., Stamford, CT, USA).

2.4. Leaf-level measurements

The 10 most ecological important evergreen broadleaf tree species from the ALS site (table 2) were selected for measurement of gas exchange and leaf sensitivity to low temperatures. The light-saturated net CO_2 assimilation rate per unit leaf area of the 10 evergreen broadleaf tree species was monitored using a portable photosynthetic system (LI-6400XT, Li-Cor Inc., Lincoln, NE, USA), during five different months (August, October, December, January and April). Six sun-exposed mature leaves from different individuals of a species were measured at a photosynthetic photon flux density of 1500 mol m^{-2} s^{-1}, at ambient temperatures and CO_2 concentrations. The measurements were conducted on sunny days between 08:30 and 10:30 h solar time, except for some August measurements conducted on cloudy days because of limited sun during the rainy season.

Leaf sensitivity to low temperatures was determined in the middle of the winter season (January 2010), when the trees were acclimated to winter temperatures, using the chlorophyll fluorescence method (Boorse *et al* 1998). Sun-exposed mature leaves from different individuals were collected in the late afternoon. The leaves were equilibrated to dark conditions by placing them in black plastic bags with wet paper towels for 12 h. Leaf samples were then exposed to a range of temperatures in a freezer: 4, 0, −2, −5, −7.5, −10, −12, −15, −17.5, −20 and −23 °C for 30 min, followed by thawing in a dark room at 15 °C for 24 h. The quantum efficiency of photosystem II (PS II) was then determined with a dual PAM-100-modulated chlorophyll fluorescence measurement system (Walz, Germany). Relative quantum efficiency was calculated as the percentage of maximum PS II quantum efficiency, which was measured at predawn under ambient conditions. The relationship between relative quantum efficiency and treatment temperature was described by a sigmoid function, which was used to determine the temperature corresponding to a 50% loss of maximum PS II quantum efficiency; this was defined as the leaf-lethal temperature of the species (LT_{50}). The p values of all regressions were <0.001.

2.5. Effects of measurement done in different years

Eddy covariance observations (2009), leaf-level measurements (2010) and soil respiration (2010–1) were done in
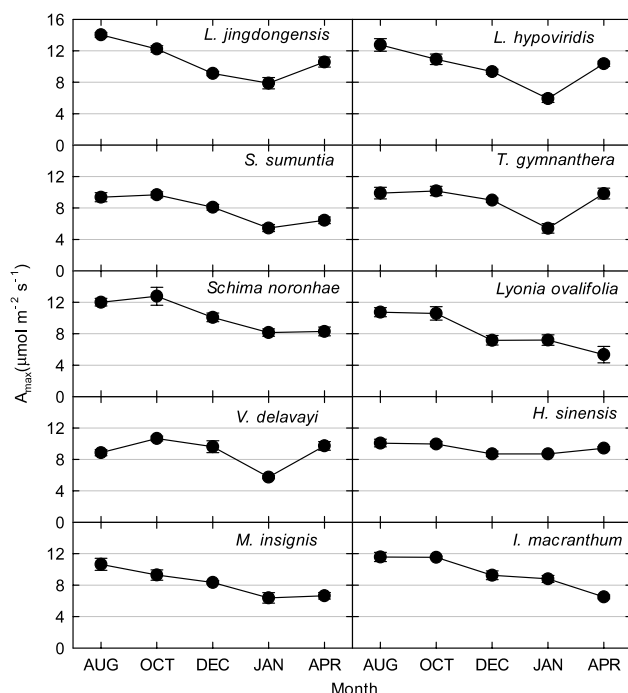
Figure 2. Seasonal dynamics of leaf maximum CO_2 assimilation ($A_{max-area}$) for 10 evergreen broadleaf species from the ALS site.

different years in the study. Nevertheless, it will not affect the analyses and conclusions. Eddy covariance data which used for inter-sites comparisons were collected from the same year of 2009. Leaf temperature sensitivity is a more genetic- than environmental-determined property. Eddy covariance observations could be confirmed by independent leaf-level measurements in different years.

3. Results

3.1. Leaf-level measurements

There was an obvious seasonal trend in leaf maximum CO_2 assimilation ($A_{max-area}$) except *H. sinensis* (figure 2). $A_{max-area}$ declined with time and approached its lowest value in late winter (January) except in *L. ovalifolia* and *I. macranthum*, which showed further decline in April. None of the $A_{max-area}$ values were less than 5 μmol m^{-2} s^{-1}, even during cold winter periods, indicating year-round photosynthetic capacity. The mean seasonal range of all species was 4.03 μmol m^{-2} s^{-1}.

The recorded temperature was never lower than the leaf-lethal temperature corresponding to 50% membrane damage (figure 3). $LT_{50\%}$ for most of the species is around $-12\,°C$. The highest $A_{max-area}$ and lowest $LT_{50\%}$ in *L. jingdongensis* may account for this species having greater importance in the community.

3.2. Soil carbon efflux

Strong seasonal pattern was observed in soil respiration (figure 4(a)). Winter soil respiration was strongly inhibited,

with a mean value of $\sim$1.5 μmol m^{-2} s^{-1}. Respiration increased rapidly during spring and peaked in summer. The dependence of soil carbon efflux on temperature can be well described by an exponential equation (figure 4(b)), from which a temperature sensitivity index (Q_{10} value) of 2.81 is derived.

3.3. Eddy fluxes

These three forest sites act as continuous, year-round carbon sinks, represented by negative values of the net ecosystem exchange (NEE) of carbon, even during winter (figure 5). At the CLS and DHS sites, the NEE is greater during cold winter months than during warm summer months, showing the opposite seasonal trend to that observed at ALS; ALS environments are more temperature sensitive than those of CLS or DHS. Both ecosystem respiration (ER) and gross ecosystem exchange (GEE) are greater during summer than winter at all three sites. There was no obvious seasonal trend in midday mean NEE of the DHS and CLS sites (figure 6). Midday mean NEE at ALS was around 12 μmol m^{-2} s^{-1} and 8 μmol m^{-2} s^{-1} in summer and winter, respectively. The light response of daytime NEE can be well fitted by Michaelis–Menten equations both in summer and winter for all three sites (figure 7). The maximum ecosystem photosynthesis rate (P_{max}) of coniferous (CLS) and mixed forest (DHS) was higher during winter than summer, whereas capacities during the winter in broadleaf forest (ALS) were lower than those in the other forest types, although still relatively high compared with rates in summer (table 3). The highest P_{max} and dark respiration (R_d) were observed at CLS, both in winter and summer (table 3). The ALS site showed greatest utilization of light under low light conditions (α) during winter. Multi-site comparisons show that ecosystem carbon-sink strength correlates inversely with mean annual temperature (figure 8): higher mean annual temperatures correlate with lower carbon-sink strengths.

4. Discussion

4.1. Continuous photosynthesis during winter

Evergreen species are not necessarily continuously photo-synthetically active throughout winter; for example, although boreal forests are evergreen, their photosynthesis is often dramatically inhibited or even halted during cold winter periods (Ottander *et al* 1995). Winter temperatures are mild in Asian subtropical areas, and subfreezing temperatures are uncommon (figure s2 available at stacks.iop.org/ERL/7/044017/mmedia). The results show that, under this climate, trees not only avoided injury during low winter temperatures, but also maintained continuous photosynthesis (figure 2). Leaf-level experimental data at the ALS site show that the historic minimum temperature was never lower than the leaf-lethal temperature corresponding to 50% membrane damage (figure 3). Although the maximum leaf CO_2 assim-ilation rates of the top-10 species (importance value) were lowest in the coldest month (except *Lyonia ovalifolia* and *I.*
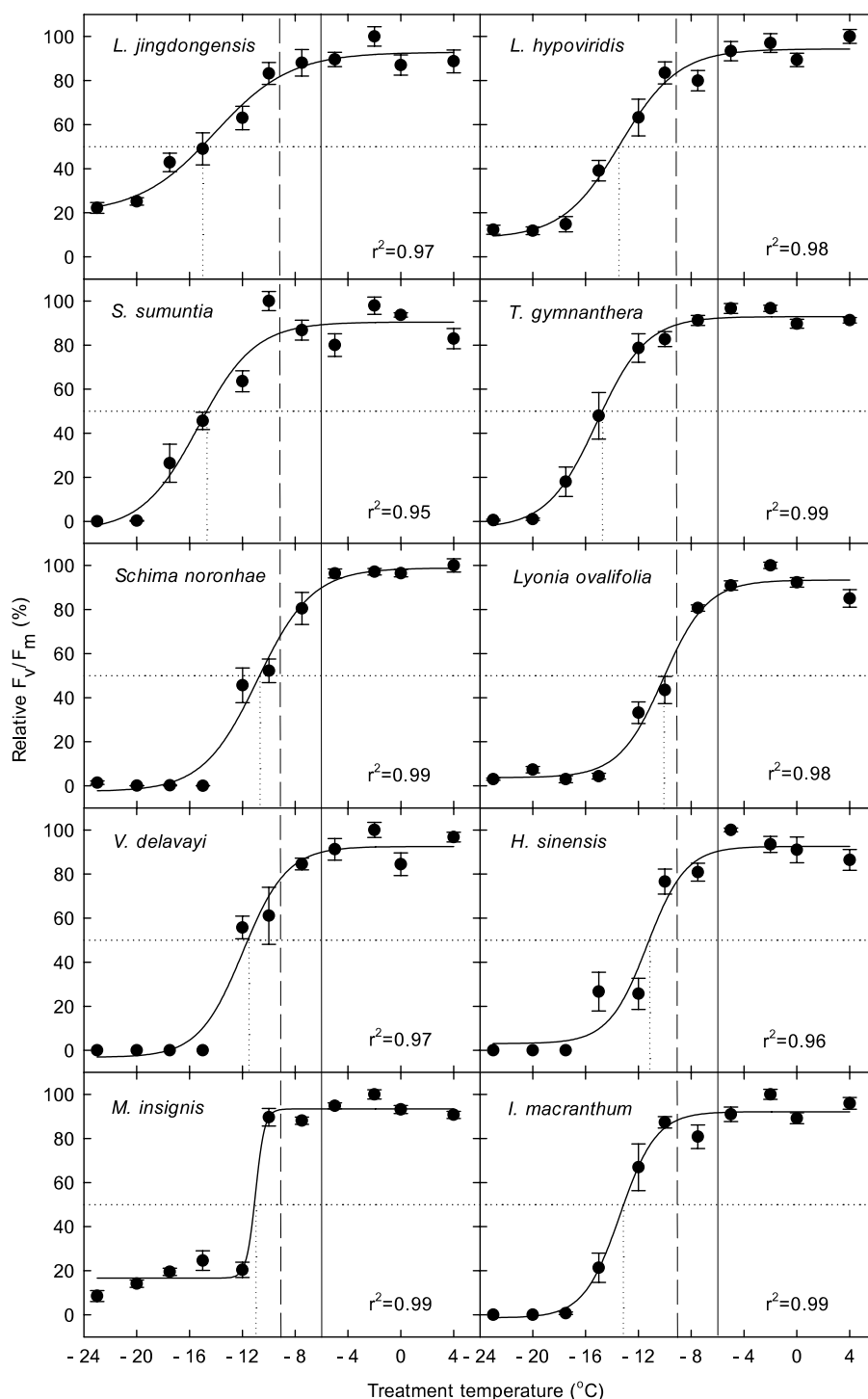
Figure 3. Relative quantum efficiency of photosystem II (PS II) as a percentage of maximum quantum efficiency of PS II (indicating percentage cell membrane or photosystem damage) for tree leaves from various species as a function of treatment temperature. Dashed lines indicate historical minimum air temperatures; dotted lines indicate leaf-lethal temperature corresponding to 50% membrane damage ($LT_{50\%}$); solid lines indicate minimum air temperatures in the 2009–10 winter season. Trends in the data were described by sigmoid functions; *p* values of all regressions were <0.001.

macranthum; figure 2), leaves maintained an assimilation rate of around 50% of peak values during this period, and never fell below 4 μmol m^{-2} s^{-1}. This finding differs from that reported for Sitka spruce (*Picea sitchensis*), which showed a very low photosynthetic rate, approaching zero, during cold periods (Neilson *et al* 1972). These are considerably high

values for carbon sequestration, as respiration losses declined strongly for low temperature (figure 4). Similar to leaf-level measurements, maximum ecosystem photosynthesis (P_{max}) at the ALS site during winter was around 50% of that during summer (figure 7; table 3). For the DHS and CLS sites, P_{max} in winter was slightly higher than in summer (table 3).
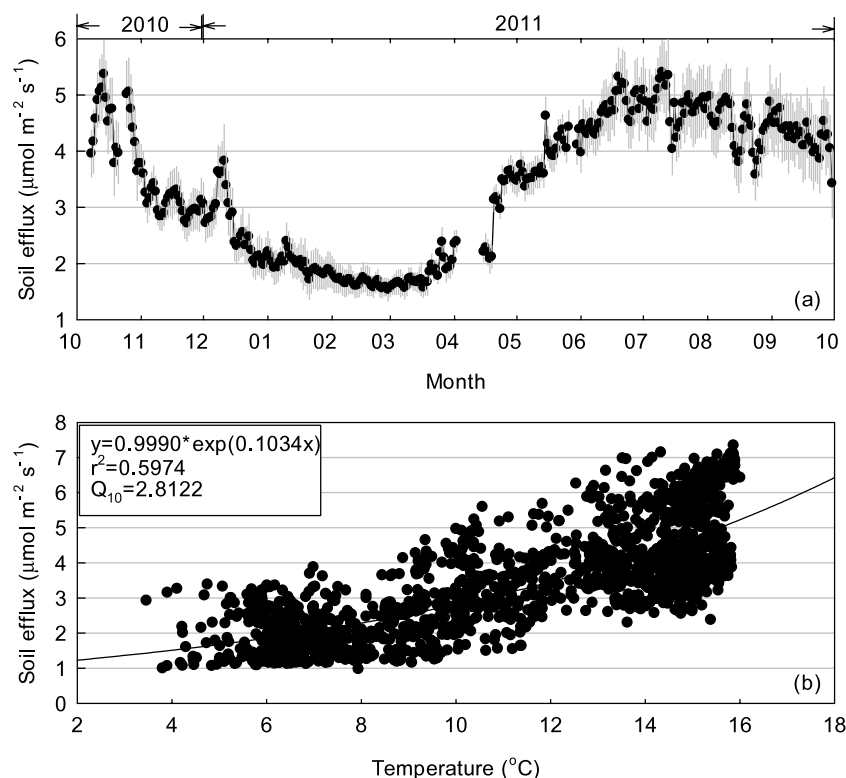
Figure 4. Daily mean soil efflux during October 2010 and September 2011 (a). Error bars are standard deviations. The dependency of respiration on soil temperature at 5 cm was fitted by a two-parameter exponential equation (b). The hourly raw data was used in regression. Q_{10} is calculated as $\exp(10*0.1034)$. $p < 0.001$ and the regression is significant.

Table 3. NEE light-response curve fitted parameters. The Michaelis–Menten equation (NEE $= -\frac{\alpha P_{max} PAR}{\alpha PAR + P_{max}} + R_d$) was used for curve fitting. Here, P_{max} is maximum ecosystem photosynthesis or ecosystem photosynthesis capacity, R_d is ecosystem dark respiration, α is apparent quantum yield to indicate the efficiency of ecosystem light utilization under low light condition. r^2 and p are determinant coefficient and regression significance, respectively.

	ALS-Winter	ALS-Summer	DHS-Winter	DHS-Summer	CLS-Winter	CLS-Summer
P_{max}	9.0671	19.557	12.5785	11.2534	21.9381	21.8871
R_d	0.1388	3.1334	1.567	2.6294	1.8868	4.6112
α	0.0541	0.0816	0.0244	0.0261	0.0336	0.0544
r^2	0.3211	0.4259	0.4079	0.3935	0.7952	0.7242
p	<0.001	<0.001	<0.001	<0.001	<0.001	<0.001

Greater P_{max} in winter observed in DHS and CLS could be caused by enhanced radiation (reduced cloudy cover) and their more low-temperature resistance needle leaf type. The annual cycle of midday mean net ecosystem exchange confirmed considerable and continuous levels of photosynthesis during winter at all three forests.

4.2. Warm summer has limited photosynthetic benefit

Gross ecosystem exchanges (GEE) of all three forests were higher in summer than in winter (figure 5). Photosynthetic rate showed limited increase at higher temperature. Mean GEE for ALS, DHS and CLS was -3.69 μmol m^{-2} s^{-1}, -2.84 μmol m^{-2} s^{-1}, -3.12 μmol m^{-2} s^{-1} in winter and -6.03 μmol m^{-2} s^{-1}, -4.14 μmol m^{-2} s^{-1}, -4.45 μmol m^{-2} s^{-1} in summer, respectively. The

highest summer-time GEE at these three sites was lower than that of the temperate deciduous forest at Harvard (~ -10 μmol m^{-2} s^{-1}) (Urbanski *et al* 2007) or the boreal aspen forest in Saskatchewan (~ -12 μmol m^{-2} s^{-1}) (Barr *et al* 2007), and were similar to that reported for the boreal black spruce forest in Manitoba, which is at the northern limit of the continuous boreal forest (~ -6 μmol m^{-2} s^{-1}) (Dunn *et al* 2007). The low summer-time GEE at the three study sites may be attributable to their evergreen phenotype, as deciduous species will enhance photosynthesis capacity under favorable conditions (Givnish 2002). The question remains of why trees do not shed their leaves during winter and then produce new leaves with higher photosynthetic capacity in order enter the summer season with improved water availability, warm climate and nutrient-rich soil contributed by litterfall; the radiation environment may account for this point. The Sun–Earth relationship would predict increased
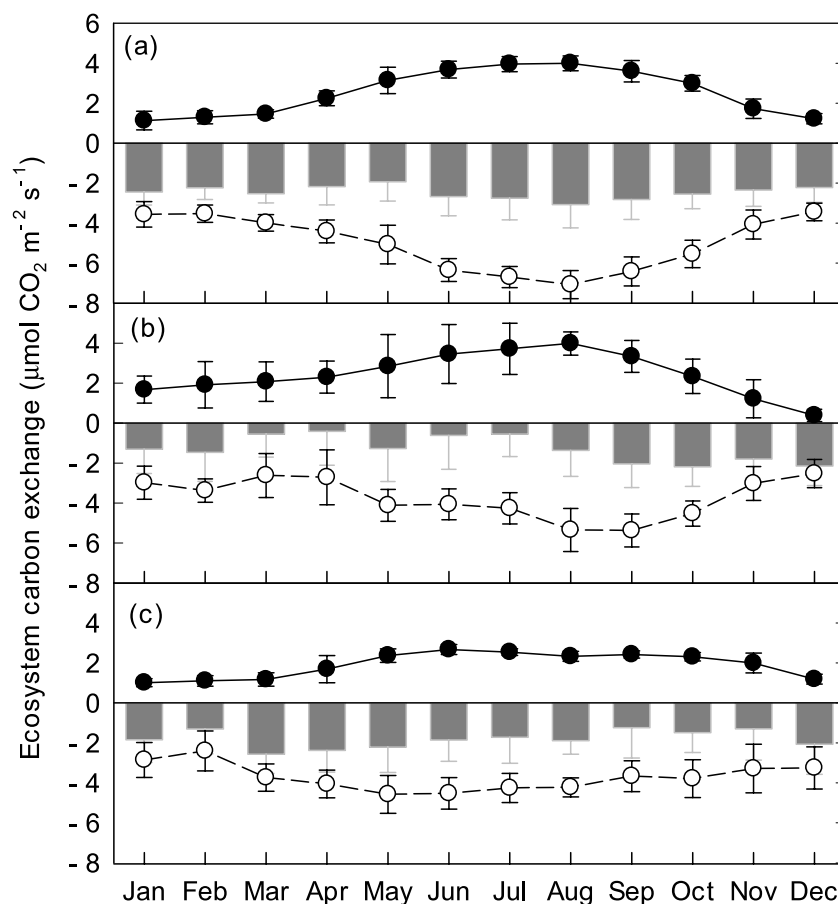
Figure 5. Monthly mean ecosystem respiration (ER, solid circles connected with solid line), gross ecosystem exchange (GEE, open circles connected with dashed line), and net ecosystem exchange (gray bars) in ALS (a), DHS (b) and CLS (c) during 2009. Error bars represent standard error of the values in each month.

radiation during summer for locations $\sim 24°$N. However, cloud formation reduced sunshine hours and, subsequently, solar radiation during summer (figure s3 available at stacks. iop.org/ERL/7/044017/mmedia). This means there is no competitive advantage for deciduous species to increase photosynthetic capacity when light is limited. As a result, GEE is higher during summer for higher temperature and abundant water conditions, but is limited in response to reduced solar radiation related to increased cloud formation.

4.3. Exponential increase of respiration with temperature

The dependence of respiration processes on temperature is well documented (Mahacha *et al* 2010, Bond-Lamberty and Thomson 2010). Soil respiration observed during warm autumns ($\sim 5\ \mu$mol m^{-2} s^{-1}) is three or four times the levels observed during winter ($\sim 1.5\ \mu$mol m^{-2} s^{-1}) (figure 4(a)). Soil respiration rates increase exponentially with temperature, as evidenced by the temperature sensitivity index (Q_{10}) value of 2.81 (figure 4(b)). The two other main determinants of soil respiration are water condition and substrate (Davidson *et al* 1998, Tang *et al* 2005). The three study forests are classed as cloud forest, with high annual rainfall and humidity (figure s3 available at stacks.iop.org/ERL/7/044017/mmedia). The annual rainfall in ALS and DHS is approximately 2000 mm,

which is similar to that of a typical rainforest (Da Rocha *et al* 2009). In comparison, annual rainfall at CLS is far greater, at >4000 mm (table 1). The annual rainfall data suggest that respiration in these forests will not be limited by insufficient water availability, even during a dry year. On the other hand, high soil carbon storage indicates that the substrate will play a minor role in limiting respiration (figure s4 available at stacks. iop.org/ERL/7/044017/mmedia). The large amounts of carbon stored in soil organic matter, forest-floor litter and coarse woody debris will provide a continuous substrate supply for respiration carbon losses; respiration will increase strongly with temperature and will not be limited by availability of water or substrate supply.

4.4. Annual temperature and carbon sequestration levels

It is very difficult to determine the major factor in the inter-sites differences observed in NEE because the three forests differ in stand age, forest type, climate, soil type and stand history (table 1). Stand age is an important factor affecting carbon balance. According to Odum (1969) succession scheme, the old-growth forest at the ALS site should be at equilibrium state or a slight carbon sink, and the 50 year-old CLS forest should show peak carbon sequestration. However, the observations were inconsistent
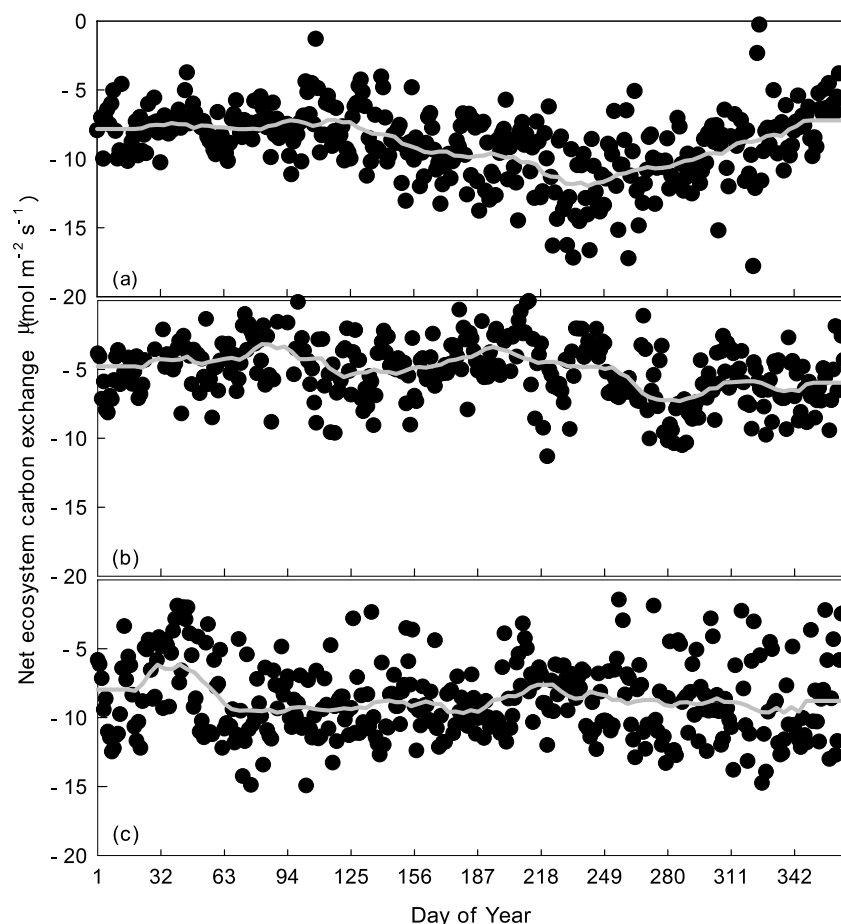
Figure 6. Temporal variation of midday mean NEE (corresponding PAR > 200 μmol m^{-2} s^{-1}) in ALS (a), DHS (b) and CLS (c). The dark gray solid line is the moving average of the dataset.
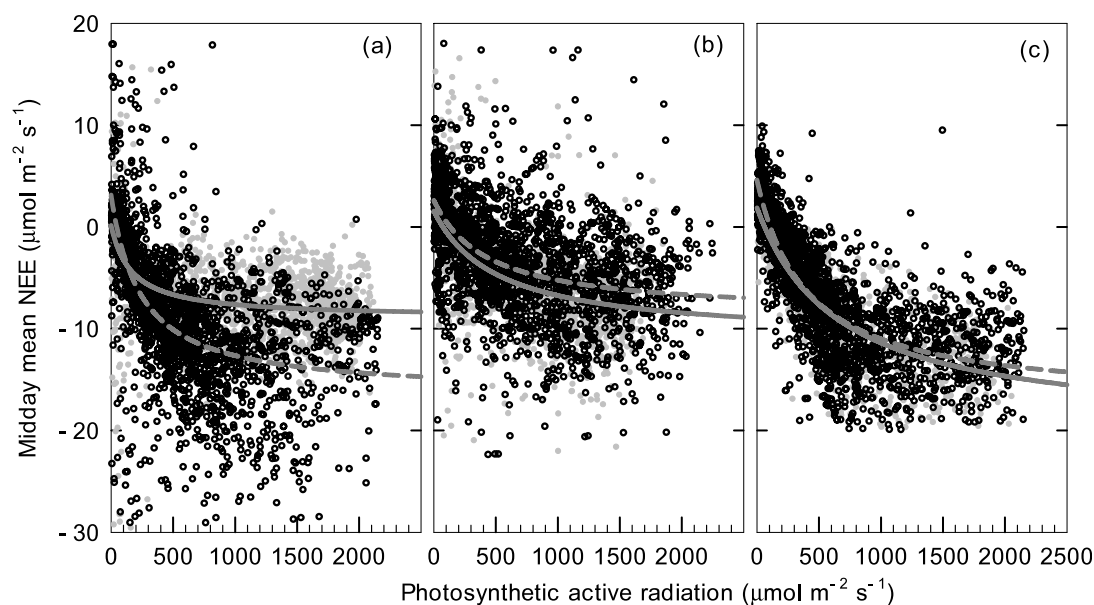

Figure 7. Light response of daytime net ecosystem carbon exchange at ALS (a), DHS (b) and CLS (c) during winter (gray circles + solid lines) and summer (open circles + dashed lines). The Michaelis–Menten equation was used to fit the light-response curves.

with such predictions. Previous studies have also reported findings that differed from those expected from the succession scheme. Observations by Kira and Shidei (1967) in temperate forests, and by Amiro *et al* (2010) and Goulden *et al* (2011) in boreal forests all indicate that NEE peaked before 40 years (mostly 20-year-old stands) and subsequently showed either
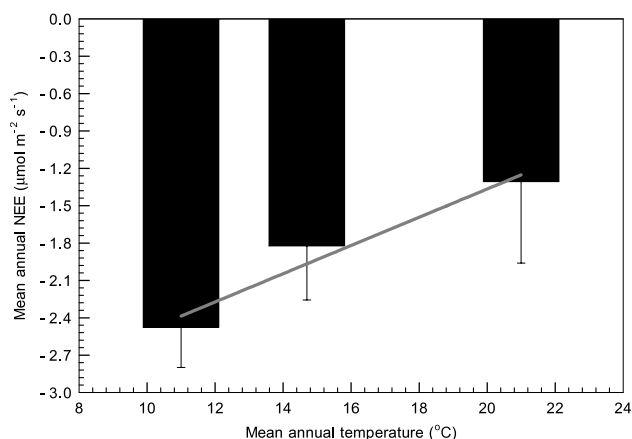
Figure 8. Mean annual NEE (net ecosystem exchange) related to mean annual temperature at the three sites. The solid line indicates a linear regression. Error bars are standard error of 365-day values.

steady state or decline. Those results suggest that the stand-age effect will be diminished in the present comparison, as the youngest stand in the study was more than 50 years old.

In terms of the explaining the species structure at a given location, Kerner von Marilaun (1898) concluded that, '*the reason for plants living together lies in the nature of the habitat*'. The three naturally established forests in the present study have interacted with their environments more than 50 years. Their current structure is nature's answer to a given environmental matrix (Körner 2003). In terms of assessing which environmental variable in the matrix plays a leading role in controlling the NEE pattern in these forests, the observation data show that neither rainfall level nor solar radiation, but rather temperature can explain the inter-site differences in NEE (figure 8; table 1). As discussed above, local rainfall is sufficient to support the ecosystems. If radiation was the dominant environmental variable, NEE at
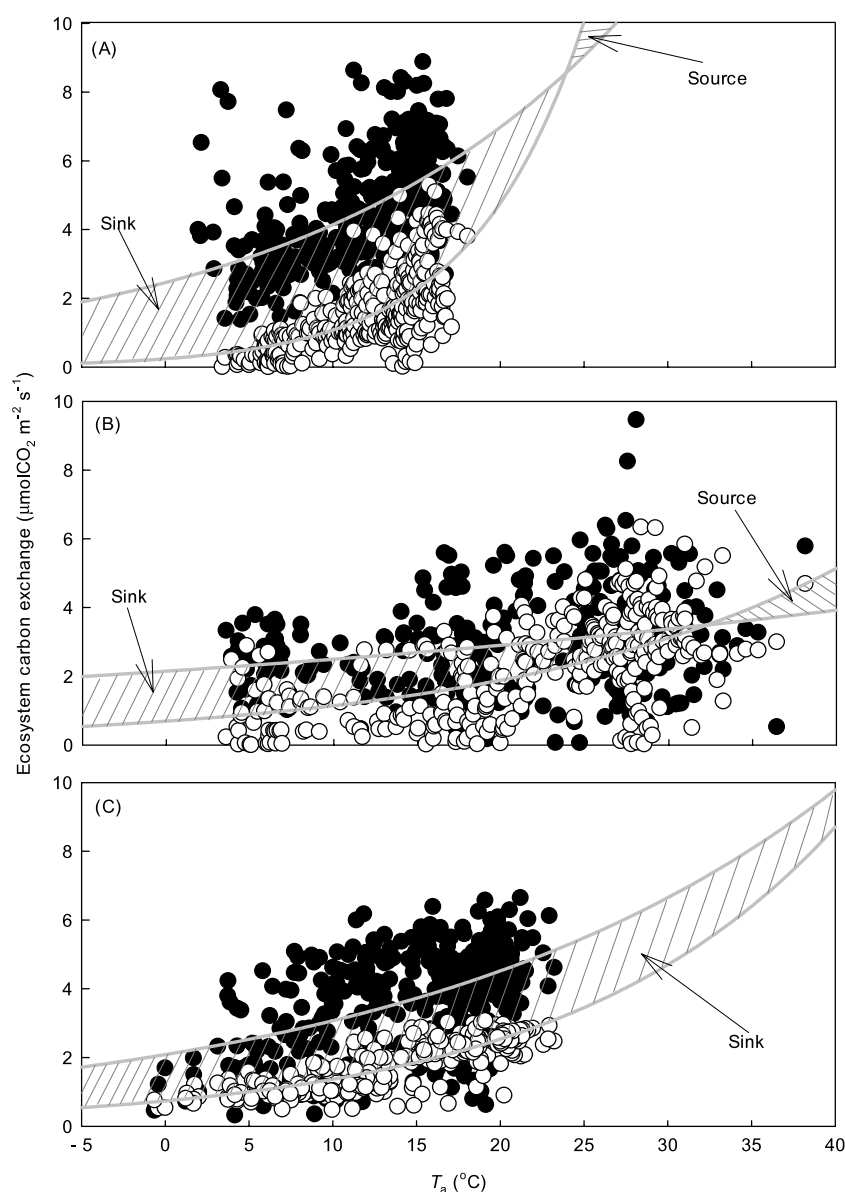

Figure 9. Assumption that temperature change produces exponential change in ecosystem respiration (open circles) and photosynthesis (solid circles); the resulting net ecosystem production (the dashed area) will be weaker with the increase of temperature. For ALS (a) and DHS (b), the ecosystem will become a carbon source above a certain temperature. For CLS (c) the sink will be weaker.

the DHS rather than the CLS site should rank second (table 1). The lowest dark respiration (R_d) was observed in the DHS forest, which had highest mean annual temperature (T_a) in addition to the lowest maximum ecosystem photosynthesis rate (P_{max}) and apparent quantum yield (α) (table 3). The ratio of P_{max} to R_d at DHS is lowest in respect to smallest NEE and highest T_a. The highest P_{max}-to-R_d ratio was found in the ALS forest, as expected. Although both P_{max} and R_d were highest in the CLS forest, the P_{max}-to-R_d ratio was moderate. Thus, temperature is key factor in the inter-sites differences in NEE.

4.5. A simple prediction

A simple prediction was made, on the assumption that both photosynthesis and respiration will increase exponentially with temperature (figure 9). As seen from figure 9, the ecosystem carbon sink (dashed area) will weaken or even convert to become a carbon source. This prediction was supported by observations. In addition, it should point out that only short-term data was collected to derive the temperature sensitivity of respiration and photosynthesis in this simple prediction. In sophistic models, the factor that longer-term temperature acclimation tends to reduce the temperature sensitivity (indicated by Q_{10}) should be considered.

Warming in East Asian subtropical evergreen forest ecosystems contributes little to photosynthesis, yet significantly increases ecosystem respiration. Consequently, warming would reduce NEE and weaken the existing carbon-sink function.

Nevertheless, temperature is only one of the factors related to regional and global climate change. Multiple other factors, including changing land-use patterns, elevated CO_2 concentrations and nitrogen deposition all function interdependently to affect ecosystem carbon balances. We have not considered elevated CO_2 in our experiments and inclusion of elevated CO_2 in our experiment could have dramatically altered the findings. Ecosystem-level manipulation experiments are necessary to track the multi-factor interactions between processes that affect ecosystem response to global or regional climate change.

Acknowledgments

References

Amiro B D *et al* 2010 Ecosystem carbon dioxide fluxes after disturbance in forests of North America *J. Geophys. Res.* **115** G00K02

Barr A G *et al* 2007 Climatic controls on the carbon and water balances of a boreal aspen forest, 1994–2003 *Glob. Change Biol.* **13** 561–76

Bond-Lamberty B and Thomson A 2010 Temperature-associated increases in the global soil respiration record *Nature* **464** 579–82

Boorse G C, Gartman T L, Meyer A C, Ewers F W and Davis S D 1998 Comparative methods of estimating freezing temperatures and freezing injury in leaves of chaparral shrubs *Int. J. Plant Sci.* **159** 513–21

Chang S-C, Tseng K-H, Hsia Y-J, Wang C-P and Wu J-T 2008 Soil respiration in a subtropical montane cloud forest in Taiwan *Agric. For. Meteorol.* **148** 788–98

Chu H S 2008 Flux measurement in the complex terrain—the Chi-Lan Mountain site *MS Thesis* National Dong-Hwa University Hualien, Taiwan

Cox P M, Betts R A, Jones C D, Spall S A and Totterdell I J 2000 Acceleration of global warming due to carbon-cycle feedbacks in a coupled climate model *Nature* **408** 184–7

Da Rocha H R *et al* 2009 Patterns of water and heat flux across a biome gradient from tropical forest to savanna in Brazil *J. Geophys. Res.* **114** G00B12

Davidson E A and Jassens I A 2006 Temperature sensitivity of soil carbon decomposition and feedbacks to climate change *Nature* **440** 165–73

Davidson R A, Belk E and Boone R 1998 Soil water content and temperature as independent or confounded factors controlling soil respiration in a temperate mixed hardwood forest *Glob. Change Biol.* **4** 217–27

Dixon R K, Brown S, Houghton R A, Solomon A M, Trexler M C and Wisniewski J 1994 Carbon pools and flux of global forest ecosystems *Science* **263** 185–91

Dunn A L, Barford C C, Wofsy S C, Goulden M L and Daube D C 2007 A long-term record of carbon exchange in a boreal black spruce forest: means, response to interannual variability, and decadal trends *Glob. Change Biol.* **13** 577–90

Givnish T J 2002 Adaptive significance of evergreen vs. deciduous leaves: solving the triple paradox *Silva Fennica* **36** 703–43

Goulden M L, Daube B C, Fan S-M, Sutton D J, Bazzaz A, Munger J W and Wofsy S C 1997 Physiological responses of a black spruce forest to weather *J. Geophys. Res.* **102** 18987–28996

Goulden M L, McMillan A M S, Winston G C, Rocha A V, Manies K L, Harden J W and Bond-Lamberty B P 2011 Patterns of NPP, GPP, respiration, and NEP during boreal forest succession *Glob. Change Biol.* **17** 855–71

Goulden M L, Munger J W, Fan S M, Daube B C and Wofsy S C 1996 Measurements of carbon sequestration by long-term eddy covariance: methods and a critical evaluation of accuracy *Glob. Change Biol.* **2** 169–82

Goulden M L, Winston G C, McMillan A M S, Litvak M E, Read E L, Rocha A V and Elliot J R 2006 An eddy covariance mesonet to measure the effect of forest age on land-atmosphere exchange *Glob. Change Biol.* **12** 2146–62

Hollinger D Y, Kelliher F M, Byers J N, Hunt J E, McSeveny T M and Weir P L 1994 Carbon dioxide exchange between an undisturbed old-growth temperate forest and the atmosphere *Ecology* **75** 134–50

IPCC (Intergovernmental Panel on Climate Change) 2007 *Climate Change 2007: The Physical Science Basis. Contribution of Working Group I to the Fourth Assessment Report of the Intergovernmental Panel on Climate Change* ed S Solomon *et al* (Cambridge: Cambridge University Press)

Johnson L C *et al* 2000 Plant carbon-nutrient interactions control CO_2 exchange in Alaskan wet sedge tundra ecosystems *Ecology* **81** 453–69

Kerner von Marilaun A 1898 *Pflanzenleben* 2nd ed (Leipzig: Bibliographisches Institut)

Kira T 1991 Forest ecosystem of East and Southeast Asia in a global perspective *Ecol. Res.* **6** 185–200

Kira T and Shidei T 1967 Primary production and turnover of organic matter in different forest ecosystems of the Western Pacific *Japan. J. Ecol.* **17** 70–87

Knorr W, Prentice I C, House J I and Holland E A 2005 Long-term sensitivity of soil carbon turnover to warming *Nature* **433** 298–301

Körner C 2003 Limitation and stress—always or never? *J. Veg. Sci.* **14** 141–3

Latta G, Temesgen H, Adams D and Barrett T 2010 Analysis of potential impacts of climate change on forests of the United States Pacific Northwest *Forest Ecol. Manag.* **259** 720–9

Liang N S, Inoue G and Fujinuma Y 2003 A multichannel automated chamber system for continuous measurement of forest soil CO_2 efflux *Tree Physiol.* **23** 825–32

Luo Y Q 2007 Terrestrial carbon-cycle feedback to climate warming *Annu. Rev. Ecol. Evol. Syst.* **38** 683–712

Mahacha M D *et al* 2010 Global convergence in the temperature sensitivity of respiration at ecosystem level *Science* **329** 838–40

Melillo J M *et al* 2002 Soil warming and carbon-cycle feedbacks to the climate system *Science* **298** 2173–6

Melillo J M *et al* 2011 Soil warming, carbon–nitrogen interactions, and forest carbon budgets *Proc. Natl Acad. Sci.* **108** 9508–12

Neilson R E, Ludlow M M and Jarvis P G 1972 Photosynthesis in Sitka Spruce (*Picea sitchensis* (Bong.) Carr.). II. response to temperature *J. Appl. Ecol.* **9** 721–45

Odum E P 1969 The strategy of ecosystem development *Science* **164** 262–70

Ottander C D, Campbell D and Quist G 1995 Seasonal changes in photosystem II organization and pigment composition in *Pinus sylvestris Planta* **197** 176–83

Piao S L *et al* 2008 Net carbon dioxide losses of northern ecosystem in response to autumn warming *Nature* **451** 49–53

Richardson A D *et al* 2010 Influence of spring and autumn phenological transitions on forest ecosystem productivity *Philos. Trans. R. Soc.* B **365** 3227–46

Schulze E-D 2006 Biological control of the terrestrial carbon sink *Biogeosciences* **3** 147–66

Tan Z-H, Zhang Y P, Schaefer D A, Yu G R, Liang N S and Song Q H 2011 An old-growth subtropical Asian evergreen forest a large carbon sink *Atmos. Environ.* **45** 1548–54

Tang J-W, Baldocchi D D and Xu L K 2005 Tree photosynthesis modulates soil respiration on a diurnal time scale *Glob. Change Biol.* **11** 1298–304

Tanner C B and Thurtell G W 1969 Anemodinometer measurement of Reynolds stress and heat transport in the atmospheric surface layer *Rep. ECOM 66-G22-F* (Madison, WI: University of Wisconsin)

Urbanski S *et al* 2007 Factors controlling CO_2 exchange on timescales from hourly to decadal at Harvard Forest *J. Geophys. Res.* **112** G02020

Wang C L *et al* 2006 CO_2 flux evaluation over the evergreen coniferous and broadleaved mixed forest in Dinghushan, China *Sci. China* D **49** 127–38

Way D A and Oren R 2010 Differential response to changes in growth temperature between trees from different functional groups and biomes: a review and synthesis data *Tree Physiol.* **30** 669–88

Webb E K, Pearman G I and Leuning R 1980 Correction of flux measurement for density effects due to heat and water vapor transfer *Q. J. R. Meteorol. Soc.* **106** 85–100

Woodwell G M, Whittaker R H, Reiners W A, Likens G E, Delwiche C C and Botkin D B 1978 The biota and the world carbon budget *Science* **199** 141–6